21, rue d'Artois, F-75008 PARIS
http : //www.cigre.org

A2-306

CIGRE 2012

BENEFITS OF TRANSFORMERS BASED ON TRIANGULAR WOUND CORE CONFIGURATIONS

T. STEINMETZ	J. SMAJIC	S.OUTTEN	T. HARTMANN	M. CARLEN
ABB	HSR	ABB	ABB	ABB
Switzerland	Switzerland	USA	USA	Switzerland

SUMMARY

Recently, dry-type distribution transformers based on triangular wound cores have been attracting increasing attention. Hence, some relevant properties of transformers based on these core configurations are analyzed in this paper in order to assess the potential benefits. Namely, no-load losses, magnetic stray fields and both current and voltage harmonics are investigated.

Numerical simulation methods to perform the no-load losses and the magnetic stray field analyses are presented and validated by measurement data. Commercial software was used to perform these 3D Finite-Element-Method based simulations. However, special modeling techniques had to be applied in order to achieve good accuracies of the simulations.

For the simulation of the no-load losses, nonlinear anisotropic material properties of the core steel laminations were considered. The low no-load losses of the investigated triangular wound core transformer according to the efficiency class B_0 is shown.

Linear material parameters were used for the simulation of the magnetic stray fields, but special care was taken in these simulations to model the surrounding air. The faster decay of the magnetic stray fields of a triangular core transformer compared to the stray fields of a planar stacked core transformer is shown by comparing the simulated magnetic fields.

Furthermore, the harmonic behavior of a triangular wound core transformer compared to a planar stacked core transformer was analyzed experimentally.

KEYWORDS

Triangular wound core - Planar stacked core - Dry-type transformer - No-load loss – Electromagnetic compatibility - Current harmonics - Voltage harmonics

thorsten.steinmetz@ch.abb.com

1. Introduction

Usually, three-phase distribution transformers feature planar core types, i.e. the limbs and the yokes of the core are coplanar. These cores can be built by either stacked or wound core standard technologies. However, these planar core configurations introduce an asymmetric component for the three-phase AC system, because the outer phases exhibit different electromagnetic properties than the center phase.

Building stacked planar cores, the core limbs and yokes are manufactured by stacking numerous straight sheets of electrical steel on top of each other. The joints where limbs and yokes are connected have to be built specially in order to keep material consumption and the core reluctance as low as possible, for instance using the step-lap technique.

Wound planar cores (e.g. Evans-cores or 5-legged-cores) usually consist of several individual bodies with different shapes. The bodies are manufactured by winding thin electrical steel foils on a mandrel. Commonly, the core bodies have to be cut and opened during the manufacturing to insert the windings on the limbs. The gap that originates from this opening of the core bodies increases the reluctance and thus the no-load losses of the corresponding transformer units.

In contrast to the planar core types, triangular wound cores as presented here consist of three identical wound core rings. These rings are manufactured by continuously winding a lamination of electrical steel on a mandrel. However, the core rings are arranged in an equilateral triangle (seen from above) in order to assemble the transformer core. All core limbs, which are formed by two adjacent rings each, are positioned at the corners of the equilateral triangle. A magnetically symmetric transformer configuration is achieved as a result.

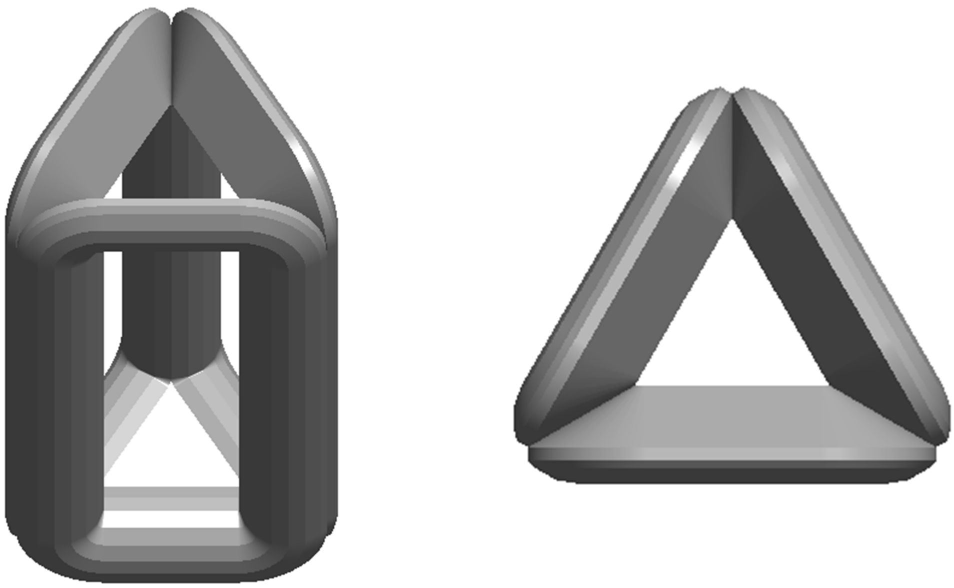

Fig.1: A triangular wound core which consists of three identical core rings. Left: perspective model. Right: model seen from above.

The core symmetry, winding arrangement, and lack of joint areas of the triangular wound cores provide various benefits over planar core types. Improvements in manufacturing techniques allow for continuously varying the width of the electrical steel lamination during the core winding process enabling an almost circular cross-sectional area of the limbs.

In the frame of this publication, different benefits of dry-type transformers using triangular wound cores are analyzed by measurements and by numerical simulations of the magneto-quasistationary fields.

2. No-load Losses

No-load losses can be analyzed by Finite-Element simulations using a field-circuit coupling: the magnetic fields in the core are represented in the field domain and coupled to an electric circuit representing the external connections of the windings to which the excitation voltage is applied. To simulate the no-load losses, the low-voltage (LV) winding, is energized at nominal voltage while the high-voltage (HV) winding is left in open-circuit.

The simulation of the electromagnetic fields is done with the commercial simulation software MagNet from Infolytica [1]. The numerical formulation [2] implemented in MagNet solves for the magnetic field $\vec{H}$ in conductive domains,

$$curl\left((\sigma + j\omega\varepsilon)^{-1}curl(\vec{H})\right) + j\omega\mu = 0,$$

and for the scalar magnetic potential Ψ in non-conductive domains,

$$div\left(\mu\left(\overrightarrow{H_s} - grad(\Psi)\right)\right) = 0.$$

In non-conductive domains, the magnetic field is then computed by $\vec{H} = \vec{H}_s - grad(\Psi)$ with $\vec{H}_s$ being a known source field.

Due to its geometrical configuration, the permeability model of the core is highly anisotropic which is challenging from the simulation point of view [3]. Considering the magnetic properties of the core bodies shown in Fig.1 it is possible to distinguish two different directions of the anisotropic permeability: (1) the intralamination direction, which has a very high magnetic permeability and which represents the flux in the winding direction of the core steel laminations, and (2) the direction of low magnetic permeability that represents interlamination flux, or flux passing between the laminations. The directions of weak magnetic properties of the core are shown in Fig.2 (right) with red arrows for different core regions.

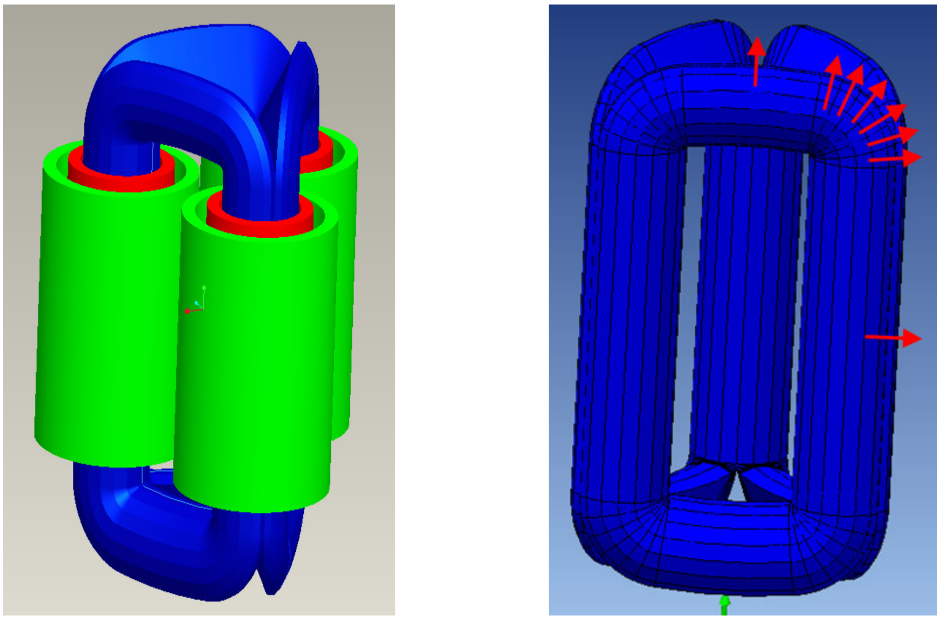

Fig.2: Left: 3-D CAD representation of a 1000kVA / 10kV triangular core dry-type transformer with high-voltage (HV, shown in green) and low-voltage (LV, shown in red) windings. Right: anisotropic core modeling using a segmentation of the core rings.

The anisotropy of the permeability μ can be considered in the simulation by using the following form of the magnetic constitutive law for the magnetic flux density $\vec{\boldsymbol{B}}$ and the magnetic field $\vec{\boldsymbol{H}}$:

$$\vec{\boldsymbol{B}} = \begin{pmatrix} \mu_{xy} & 0 & 0 \\ 0 & \mu_{xy} & 0 \\ 0 & 0 & \mu_z \end{pmatrix} \vec{\boldsymbol{H}}$$

Evidently, considering Fig.2, the direction of weak magnetic permeability is position dependent and it would be ideal to define the magnetic permeability tensor as a corresponding spatial function. Unfortunately, in the commercial field software used for the presented electromagnetic simulations (Infolytica MagNet), this capability has not been implemented up to now. Instead, it is possible to define a constant permeability tensor and assign it to a certain body with respect to its local Cartesian coordinate system. Therefore the core bodies were geometrically split and over each core element a single but constant magnetic permeability tensor was specified. The core splitting segments are shown in Fig.2 (right).

The nonlinear BH-curve of the used core material is defined in the direction of the strong magnetic properties of the core (μ_{xy}). In the weak direction perpendicular to the lamination, a low value of the magnetic permeability $\mu_z$is assumed and its value estimated according to an extensive numerical study involving measured comparison data.

This process results in a robust and reliable simulation setup that requires intensive preprocessing work (CAD modeling of the split core) yielding reliable results in the end. The simulation results, i.e. the distribution of the magnetic flux density and the iron loss density, are presented in Fig.3.

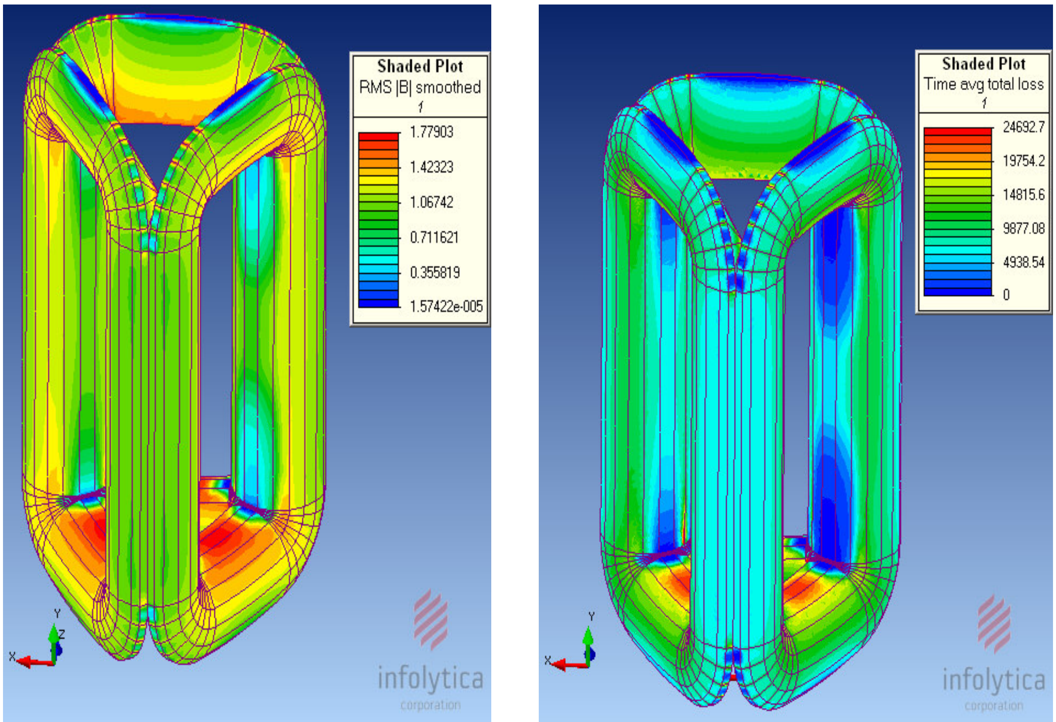

Fig.3: Results of the no-load simulation of the triangular core transformer (shown in Fig.2). Left: magnetic flux density distribution in Tesla. Right: Core loss density in Watt.

Evidently, as a result of the splitting and anisotropic modeling, some core regions have a deeper saturation level than they do in reality. For example, the innermost part of the yokes reaches the RMS value of 1.8T which is too high and thus unrealistic. However, these regions are small in terms of volume and do not affect significantly the overall simulation accuracy.

The magnetic flux distribution in the rest of the core rings is accurate resulting in the total core losses of 1156W. The corresponding measured value was 1483W [4] which is within the no-load loss requirement for the B_0 efficiency class [5]. The simulated core losses are lower than the measured ones, which is plausible due to the fact that the material loss curve of the steel grade is used for computing the core losses in the simulation. This material curve cannot consider the deterioration of the iron losses of the steel due to the manufacturing process. Thus, measured losses must be higher than simulated (or calculated) losses. Commonly, this effect is taken into account in the transformer design by the core building factor. The above values give a building factor of 1.28, which is a value in the range of typical building factors for this kind of products. Thus, it can be concluded that the simulation has reached a good accuracy. This accuracy can be improved further by introducing local loss correction factors that can be determined by empirical testing.

After testing the algorithm, the complete process is automated by writing VisualBasic scripts describing repetitive tasks within the field solver used (Infolytica MagNet). If the splitting of the core geometry is done properly and if the mesh generated has a reasonable quality the convergence of the nonlinear anisotropic magnetic simulation is very fast. The CPU time of the simulation presented in Fig.3 is below one hour on a modern multi-core workstation machine.

3. Stray Field Emissions

The operation of transformers near to sensitive areas, i.e. inhabited areas with long-term human presence (not in professional environment), may require low emission of unintentional stray fields. In Switzerland, for example, the maximum permissible magnetic stray flux density of transformers, operated at 50Hz in sensitive areas, is limited to 1µT [6]. Dry-type transformers are, due to their high operating safety, very suitable to be operated in sensitive areas like apartment houses, schools or hospitals. Thus, an electromagnetic compatibility (EMC) study is performed to assess the magnetic stray fields of a triangular core dry-type transformer.

This EMC study is performed by both simulations and measurements of a 1000kVA, 12kV unit under the load setup. This means that the primary windings are energized at reduced voltage while the secondary winding system is connected in short-circuit. The applied voltage is reduced so that nominal currents flow in both winding systems.

The simulation setup is based on a 3D model of this transformer [7] including core, windings, clamping structure and parts of the LV busbars. Linear material behavior is assumed in the whole model, because the magnetic core is only slightly magnetized due to the Ampere-turn balance of the winding systems. Finite-element simulations of magnetic fields require the active part of the simulation domain to be embedded into an appropriate airbox and that reasonable boundary conditions at the boundary faces of the airbox are set. Both are needed to ensure that the simulated fields mimic the asymptotic behavior of the vector fields realistically. For the simulation of stray field emissions, special care has to be taken of the airbox surrounding the transformer, because the simulated fields have to be evaluated exactly there. Thus, the active part of the transformer is embedded into at least two different airboxes. On the one hand, the inner airbox is finely discretized and usually second-order polynomial shape functions are used, which allow for an accurate evaluation of the magnetic stray fields in this region. On the other hand, this fine level of discretization is not needed outside of the evaluation domain. Thus, the outer airbox is large enough to allow for a realistic asymptotic behavior of the magnetic fields, but has coarser mesh size and first-order polynomial shape functions to reduce the computational effort.

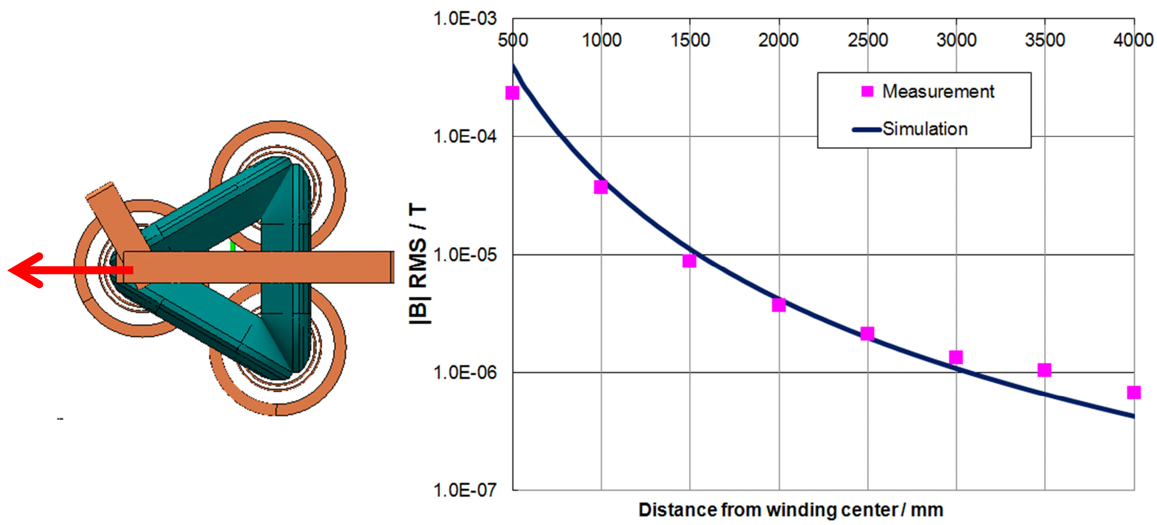

Fig.4: Comparison of measured and simulated magnetic stray fields.

Furthermore, the magnetic stray fields are also measured using a low-frequency SPECTRAN NF spectrum analyzer. The measured flux density RMS values are compared against the simulations in Fig.4. The evaluation is done along a straight line indicated by the red arrow in the figure. The origin of the line coincides with the center of the windings as shown. The evaluation height is at the vertical center of the windings.

As demonstrated, the magnetic stray fields can be assessed by simulations accurately. To show the benefit of reduced stray fields of a triangular core transformer over a planar stacked core, a planar core transformer with the same power and voltage rating as the triangular core transformer is simulated. To assess the influence of the core type on the stray fields, only core, windings and clamping structure are considered. The LV busbars, HV cables and other conductors are not taken into account in the simulation models. Fig.5 and Fig.6 show the results of the simulations.

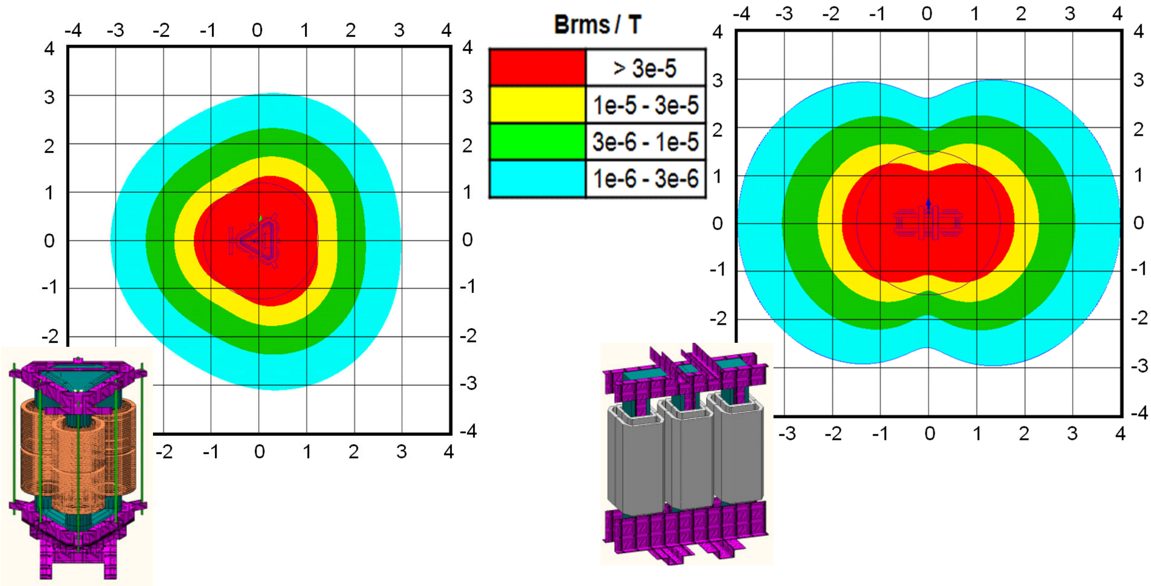

Fig.5 : Comparison of the magnetic stray fields. Left: triangular core transformer. Right: planar core transformer. View from the top is shown. The length scale is in meters. The evaluation of the magnetic flux density is done at the vertical centers of the windings.

The figures show that the magnetic stray field of the triangular core transformer decay faster below the 1μT limit than the stray fields of the planar stacked core unit, i.e. the required clearance distance is smaller. Thus, the triangular core transformer shows a better EMC performance which makes it attractive for operation in sensitive areas.

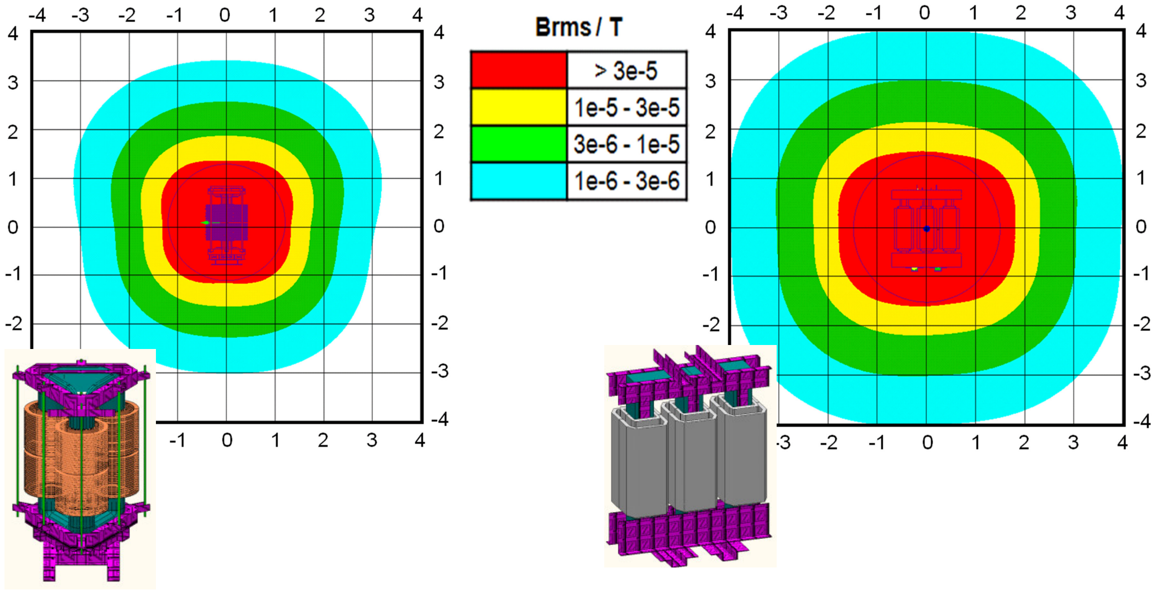

Fig.6 : Comparison of the magnetic stray fields. Left: triangular core transformer. Right: planar core transformer. View from the side is shown. The length scale is in meters. The evaluation of the magnetic flux density is done through the centers of the transformers.

The better EMC performance of the triangular core transformer can be explained by the compact and symmetric configuration of both the core geometry and the excitation of the windings. It allows the stray fields of the different phases to cancel and decay closer to the triangular unit than for a bilaterally symmetric planar transformer.

4. Harmonic Behavior

To determine the excitation current behavior, a 500 kVA / 10kV triangular core transformer was compared against a stacked planar unit with similar ratings.

The harmonics of the excitation current are measured in each phase of the excitation line with current transformers connected to a Yokogawa harmonic analyzer. Each phase is measured individually, and the average magnitude is calculated for each harmonic. The harmonics measured are 1 (Primary) through 20. The current and voltage harmonics are measured for each unit. The results of the measurement are shown in Fig.7.

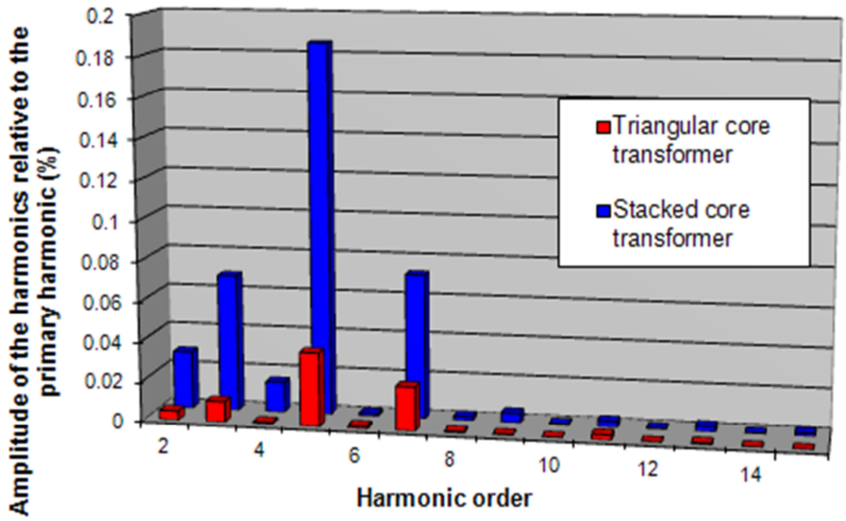

Fig.7: Current harmonic comparison of the triangular core transformer against the planar stacked core unit.

As can be seen from the current harmonic comparison, the third harmonic is reduced in comparison to the stacked core unit, and less significant, but present differences can be seen with sixth and ninth harmonics. In addition, there is a strong reduction in the fifth and seventh harmonics, but this is partially an effect of the excitation level as can be seen in Fig.8.

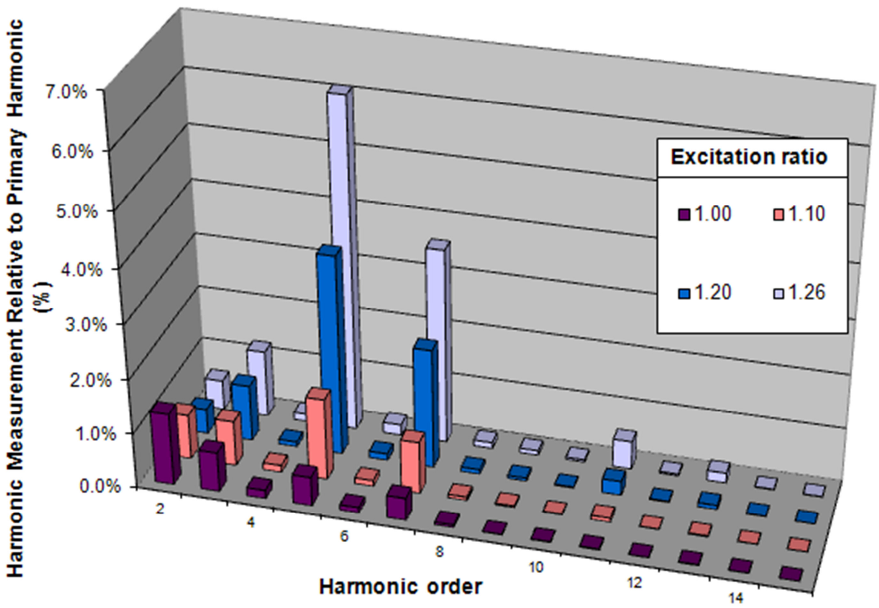

Fig.8 : Current harmonic per unit excitation (triangular core transformer).

As can be seen in the above figure the harmonic contribution from the fifth and seventh harmonic increases as core excitation increases and saturation is approached, but this increase is not seen in the third harmonic.

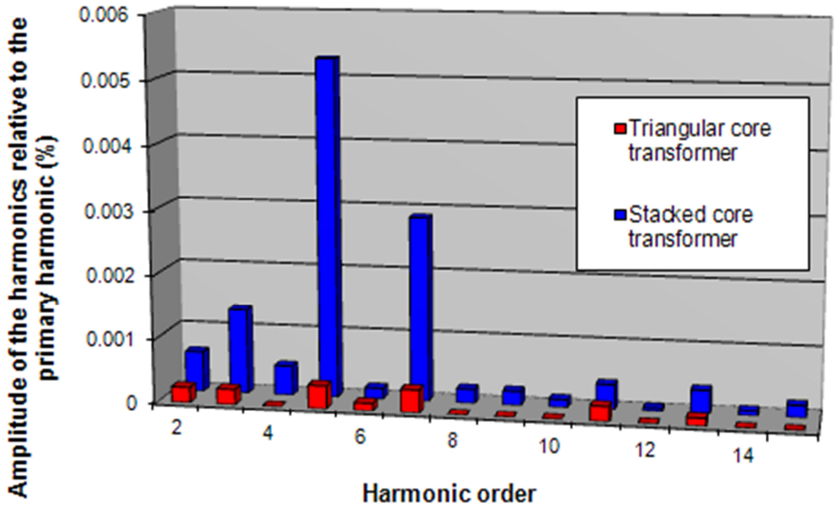

Fig.9: Voltage harmonic comparison (100% excitation) of the triangular core transformer against the planar stacked core unit.

The comparisons in the voltage harmonics revealed similar phenomena to that of the current harmonics, in that the third harmonic is reduced from the stacked core unit. This voltage harmonic has a similar behavior to the current harmonic as the unit excitation increases, in that the fifth and seventh harmonics increase, but no substantial change is seen in the third harmonic.

From the measured harmonic results, it can be seen that triangular core transformers experience (1) a reduction in the third harmonic that persists through multiple excitation levels, and that (2) nominal excitation levels experience a further reduction in harmonic behavior in comparison to stacked core units.

5. Conclusion

The analyses presented in this paper show various benefits of transformers featuring triangular wound cores: low no-load losses, reduced EMC relevant magnetic stray fields and improved harmonic behavior are advantages of these transformers compared to planar stacked core transformers of corresponding ratings.

Numerical simulations are presented for computing no-load loss and magnetic stray fields of triangular core transformers. A good accuracy of the simulations is found by validation of the computed data against measurements. The accuracy of the no-load loss simulations can be improved further by investigating core building factors applicable to triangular wound core configurations.

Finally, also the current manufacturing technologies have contributed to the development of efficient transformers based on triangular wound core configurations.

BIBLIOGRAPHY

[1] Infolytica MagNet: Design and Analysis Software for Electromagnetics, www.infolytica.com, Infolytica Corporation.

[2] J. P. Webb, B. Forghani, "A T-Omega method using hierarchal edge elements" (IEE Proceedings, Sci. Meas. Technol., Vol. 142, No. 2, 1995)

[3] T. Steinmetz, B. Cranganu-Cretu, J. Smajic, “Investigations of no-load and load losses in amorphous core dry-type transformers” (XIX International Conference on Electrical Machines (ISEM), 2010, ISBN 978-1-4244-4174-2)

[4] International Standard IEC 60076-1, “Power Transformers – Part I” (Edition 2.1, 2000)

[5] European Standard EN-50541-1, "Three phase dry-type distribution transformers 50 Hz, from 100 to 3150 kVA, with highest voltage for equipment not exceeding 36 kV - Part 1: General requirements" (2010)

[6] “Ordinance relating to Protection from Non-Ionising Radiation” (Swiss Corpus Juris, SR 814.710, 1999)

[7] J. Smajic, T. Steinmetz, B. Cranganu-Cretu, A. Nogues, R. Murillo, J. Tepper, “Analysis of near and far stray magnetic fields of dry-type transformer: 3-D simulations versus measurements” (IEEE Transactions on Magnetics, Vol. 47, Iss. 5, 2011)